

June 13, 2006.

# Wavelets and Solar Magnetic Activity I: Wavelets on the Edge

Robert W. Johnson

*Fusion Research Center, Georgia Institute of Technology, Atlanta, GA 30332, USA*

`rob.johnson@gatech.edu`

## ABSTRACT

The traditional continuous wavelet transform is plagued by the cone-of-influence, *ie* wavelets which extend past either end of a finite timeseries return transform coefficients which tend to decrease as more of the wavelet is truncated. These coefficients may be corrected simply by rescaling the remaining wavelet. The corrected wavelet transform displays no cone-of-influence and maintains reconstruction as either edge is approached. As an application and example, we present the edge corrected wavelet transform of the (derectified) yearly International Sunspot Number,  $R_i$ , as a measure of solar magnetic activity, and compare the yearly solar magnetic power with Oerlemans' glacial global temperature reconstruction.

*Subject headings:* wavelet, cone-of-influence, CWT, sunspot, solar activity, global temperature

## 1. Introduction

The continuous wavelet transform, or CWT, as traditionally defined (see Torrence & Compo (1998) for a practical guide):

$$W(s, t) \propto s^{-\frac{1}{2}} \int_{-\infty}^{\infty} \Psi^* \left( \frac{t - t'}{s} \right) f(t') dt' \quad (1)$$

suffers from a decline in its response as the analyzing wavelet runs off either edge of a finite timeseries of data. This region, where the CWT coefficients decrease, is known as the cone-of-influence. For the complex Morlet wavelet

$$\Psi_0(t) \propto e^{i\omega_0 t} e^{-\eta^2/2} \sim h(t)\Phi(t) \quad (2)$$

where  $\eta = \left(\frac{t-t'}{s}\right)$ , and  $\Phi(t) = e^{-\eta^2/2}$  is the scaling function, one may rescale wavelets on the edge by normalizing to unity the integral of the scaling function remaining over the data (assuming unit normalization for the untruncated scaling function). Let  $t$  be defined on unit intervals;  $t \rightarrow t_j$  for  $j \in [1, \dots, N]$ . For an untruncated support width on the interval  $[1, 2k+1]$  and location  $1 \leq \tau \leq k$  from the left edge, one takes

$$W(s, \tau) \rightarrow W(s, \tau) \left( \frac{\sum_1^{2k+1} \Phi(t_j)}{\sum_1^{k+\tau} \Phi_\tau(t_j)} \right) \quad (3)$$

and similarly for the right edge. While not investigated in this paper, a similar approach should hold for wavelets spanning finite gaps in a timeseries. Unlike adaptive wavelets, Frick et al. (1997), and the lifting scheme of Sweldens (1998), this technique preserves the shape (if not the moments) of the analyzing wavelet regardless of the distance to the edge. While similar in response to the weighted wavelet transform of Foster (1996), this approach is far simpler to implement.

## 2. Analysis of Solar Magnetic Activity

### 2.1. Edge Corrected Wavelet Transform Power Spectral Density

To demonstrate the corrected wavelet transform, we analyze the timeseries of sunspot data given by the International Sunspot Number,  $R_i$ , at the Solar Influences Data Analysis Center by der Linden & the SIDC team (2005). Following Buck & Macaulay (1993) and the observation by Hale that the sunspot number should represent a rectification of the underlying solar magnetic activity, we derectify the signal by taking the square root of  $R_i$  and inserting alternating signs as appropriate

$$R_i(t_j) \rightarrow \pm \sqrt{R_i(t_j)} \quad (4)$$

The familiar yearly sunspot numbers  $R_i$  are shown in Figure 1, and the derectified values  $\pm \sqrt{R_i}$  are displayed in Figure 2. With derectification, the sunspot Schwabe cycle of  $\sim 11$  years is seen to correspond to the magnetic Hale cycle of  $\sim 22$  years.

The uncorrected wavelet power spectral density is shown in Figure 3. The cone-of-influence is indicated by the dashed black line. Coefficients within the triangle formed by the black line and the upper axis (the triangle-of-validity?) are not affected by wavelet truncation; the rest are. As the dominant cycle lies mostly outside the triangle-of-validity, one cannot trust quantitative calculations using these coefficients. The effect is clearest at the edges of the transform, as the amplitude of the dominant cycle certainly should not

disappear as one approaches the present! We see the effects of the cone-of-influence on signal reconstruction as a decline in the reconstructed amplitude as the edge of the timeseries is approached in Figure 5. For the edge corrected wavelet transform, Figure 4, no cone-of-influence is seen, and perfectly adequate reconstruction is maintained out to the edge of Figure 5. Note that the difference in the transforms is best seen in the online color versions of the figures.

## 2.2. Harmonic Analysis

One may integrate the wavelet power spectral density along the time axis to find the mean harmonic content contained in the signal, Figure 6. Here one clearly sees the dominant cycle at  $\sim 22$  years, as well as the third harmonic at  $\sim 7$  years, in agreement with Buck & Macaulay (1993). The fifth harmonic also seems to be represented in the mean harmonic content. Looking back at the wavelet power spectral density, Figure 4, one can see intermittent activity at shorter scale lengths, corresponding to higher harmonics, as well as activity at longer scale length modes.

## 2.3. Solar Magnetic Power vs Global Temperature

One may integrate the wavelet power spectral density along the scale axis to find the yearly solar magnetic power, Figure 7. Here one sees a gentle oscillation in the two centuries following the Maunder Minimum, followed by a clearly increasing level of activity throughout the 20th century. Plotted alongside is Oerlemans (2005) glacial reconstruction of the global temperature “anomaly”, defined as the difference from the mean temperature of some years around 1950. Again, gentle oscillations are followed by a clear warming trend in the 20th century. As the solar dynamo is powered by convective (and other?) flows within the sun, Lawrence et al. (1995), an increase in solar magnetic activity might well correlate with an increase in solar irradiance, with climatic consequences here on Earth.

## 3. Conclusions

By rescaling the wavelets on the edges of a timeseries of data, one may construct a corrected wavelet transform which has no cone-of-influence and maintains reconstruction. Applying the corrected wavelet transform to the solar magnetic activity as recorded in sunspot data, a clearly increasing level of activity is seen during the 20th century. A correlation

with global temperature is observed. We note that the corrected wavelet transform may be further enhanced, Johnson (2006), to reveal more detailed information about the yearly harmonic content of the solar magnetic activity record.

## REFERENCES

Buck, B., & Macaulay, V. 1993, in Maximum Entropy and Bayesian Methods, ed. A. Mohammad-Djafari & G. Demoments (Netherlands: Kluwer Academic Publishers), 345–356

der Linden, R. V., & the SIDC team. 2005, online catalogue of the sunspot index

Foster, G. 1996, *The Astronomical Journal*, 112, 1709

Frick, P., Baliunas, S., Galygin, D., Sokoloff, D., & Soon, W. 1997, *ApJ.*, 483, 426

Johnson, R. W. 2006, in APS Conference Proceedings, April 22-26, Dallas, TX, American Physical Society

Lawrence, J. K., Cadavid, A. C., & Ruzmaikin, A. A. 1995, *ApJ*, 455, 366

Oerlemans, J. 2005, *Science*, 308, 675

Sweldens, W. 1998, *SIAM Journal on Mathematical Analysis*, 29, 511

Torrence, C., & Compo, G. P. 1998, *Bulletin of the American Meteorological Society*, 79, 61

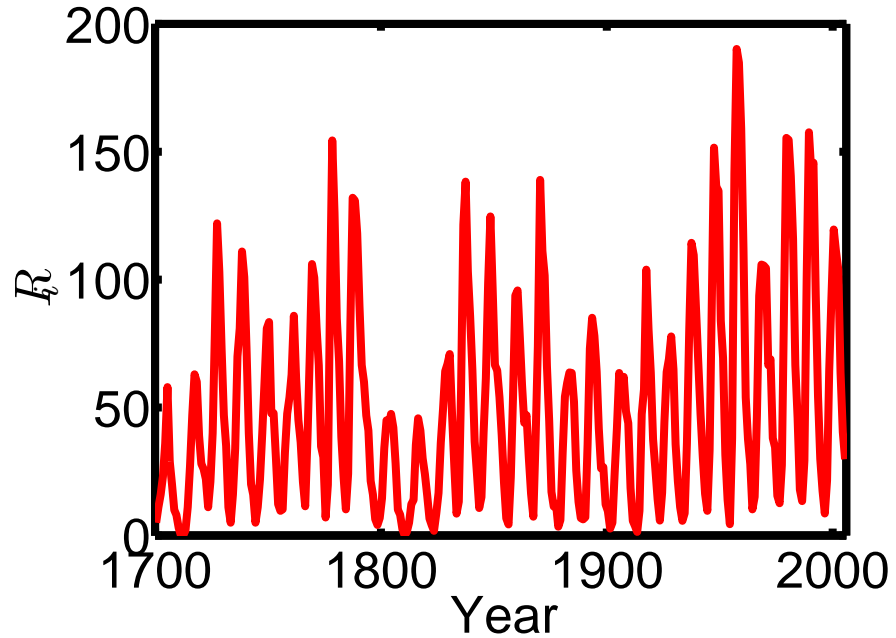


Fig. 1.— International Sunspot Number  $R_i$ . credit: SIDC, RWC Belgium, World Data Center for the Sunspot Index, Royal Observatory of Belgium.

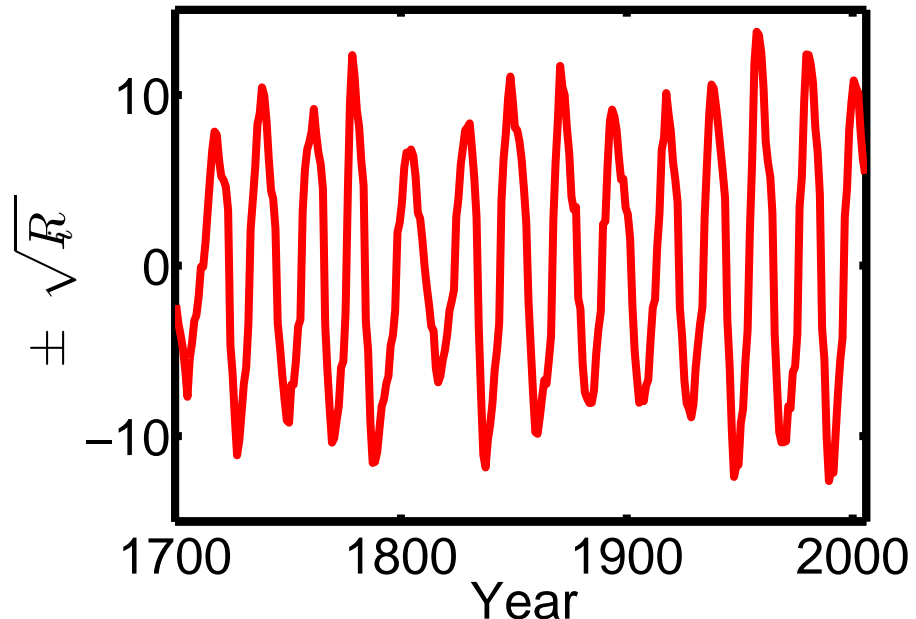


Fig. 2.— Derectified Sunspot Number  $\pm\sqrt{R_i}$ .

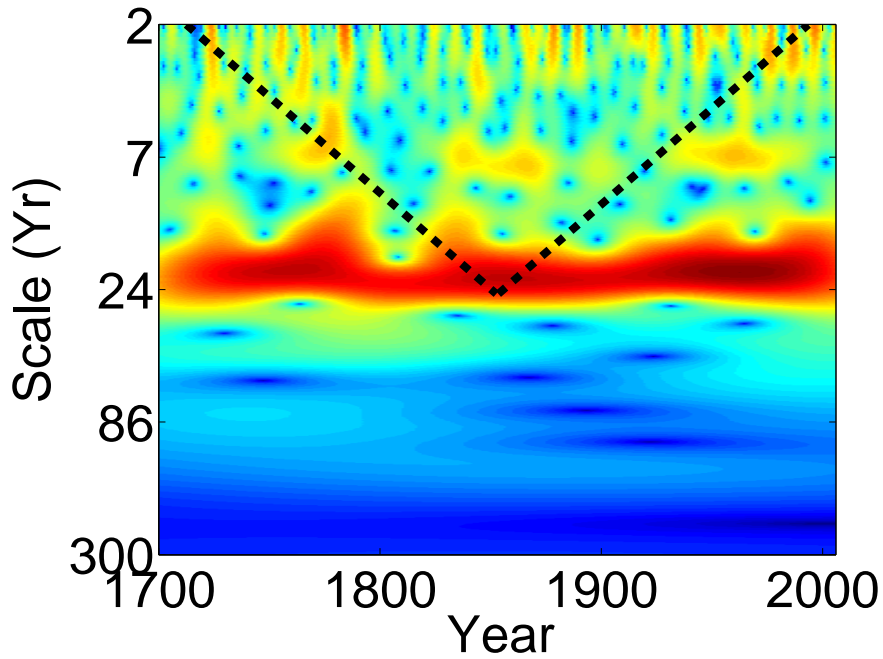


Fig. 3.— Conventional Wavelet Transform PSD. Color version available online.

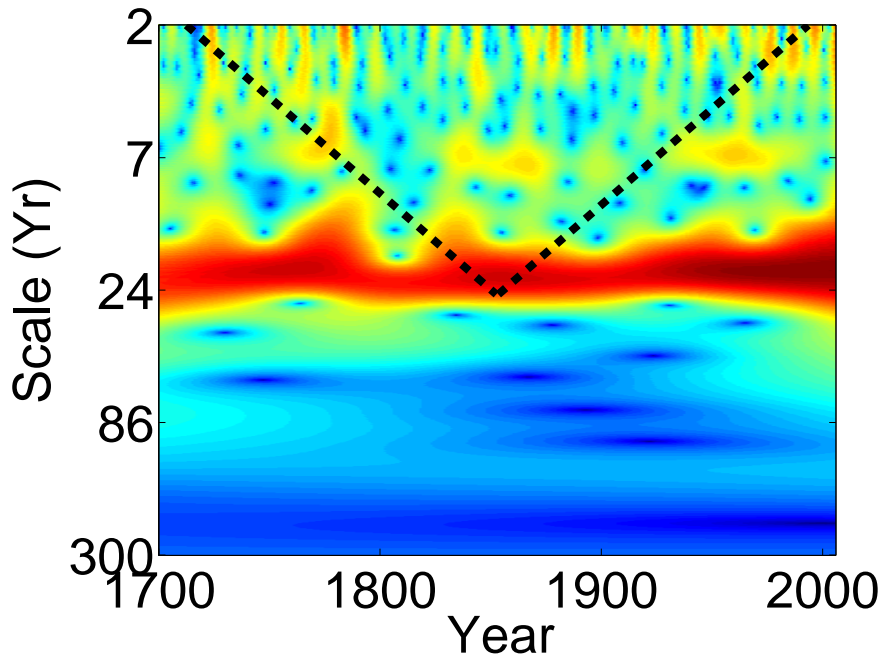


Fig. 4.— Edge Corrected Wavelet Transform PSD. Color version available online.

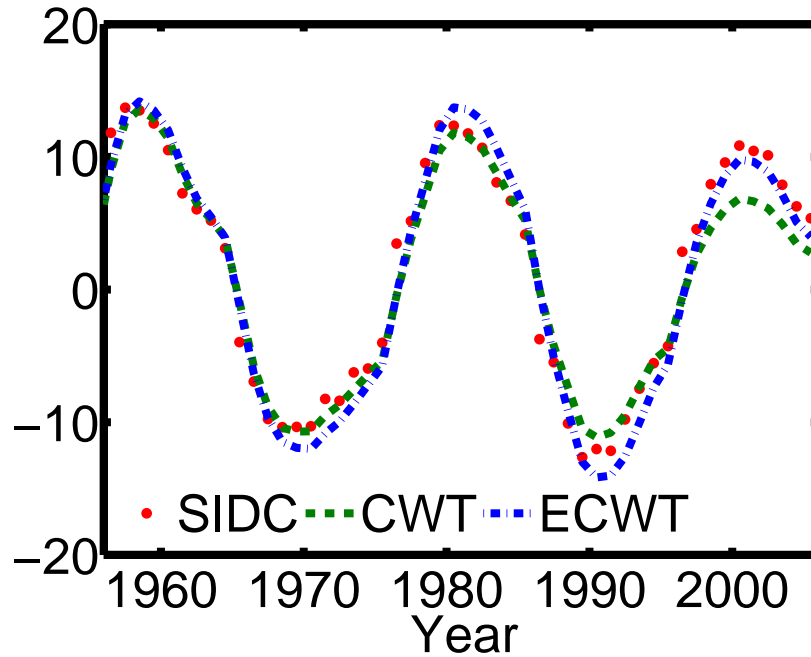


Fig. 5.— Signal Reconstruction.

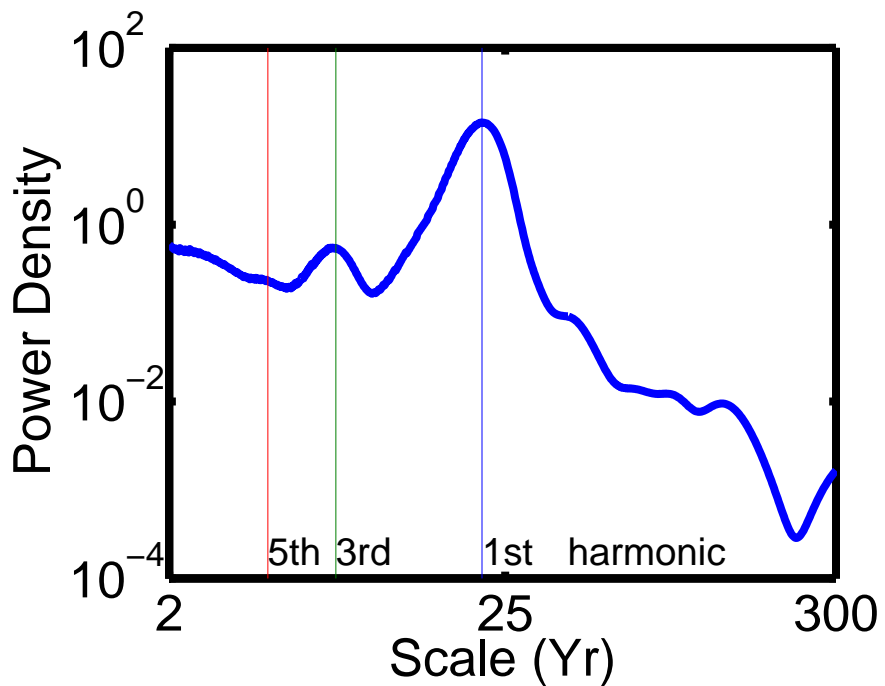


Fig. 6.— Mean Harmonic Content.

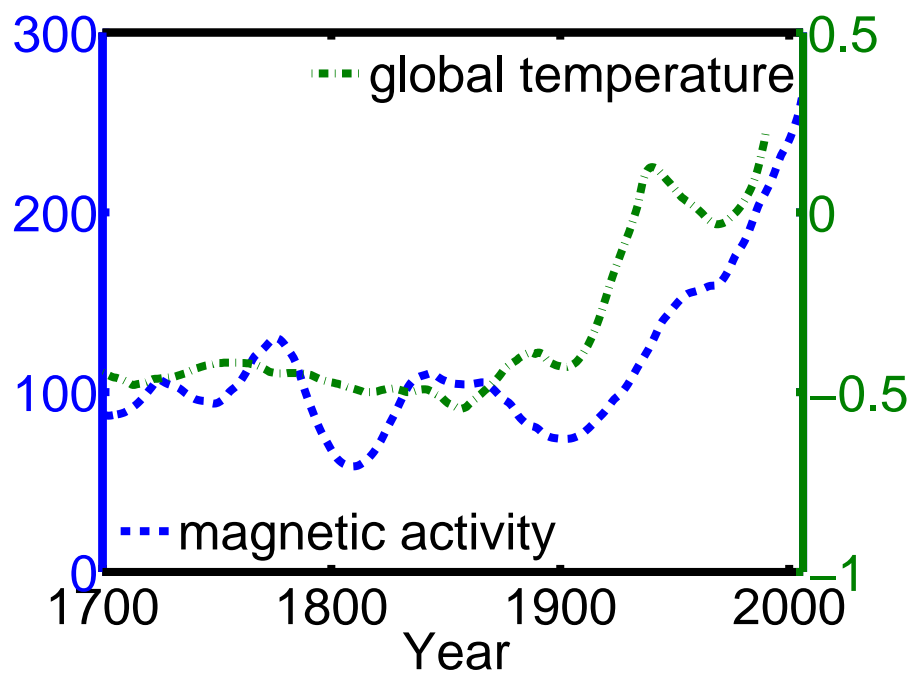


Fig. 7.— Yearly Solar Magnetic Activity vs Global Temperature.